Oxidation and unzipping in ELIUM resin: Kinetic model for mass loss

Mohamed Souheib Chebil [a], Guillaume Bouaoulo [a], Pierre Gerard [b], Salma EL Euch [c], Hervé Issard [c], Emmanuel Richaud [a,*]

[a] Laboratoire PIMM, Arts et Metiers Institute of Technology, CNRS, Cnam, HESAM University, 151 boulevard de l'Hopital, 75013, Paris, France.
[b] Arkema, Laboratoire Composites, Groupement de Recherche de Lacq, 64170, Lacq, France.
[c] ORANO TN, 1 rue des Hérons, 78180, Montigny-le-Bretonneux, France.

ARTICLE INFO

ABSTRACT

This paper gives a first study of the thermal and thermal oxidative ageing of ELIUM® resins. Chain ends unzipping was observed to be the main degradation mechanism under nitrogen whereas an oxidation mechanism with random chain scissions is shown to predominate in presence of oxygen. A first simplified kinetic model is proposed and fits experimental results for thin films at temperatures ranging from 230 to 310°C under oxygen or nitrogen.

© 2021 Elsevier Ltd. All rights reserved.

1. Introduction

Manufacturing of large composite parts with short processing times, low external heating is a continuous challenge in several industrial sectors such as marine industry (hull and bridges of race boats), aeronautic and aerospace industry, renewable energy (wind turbine blade) [1].

ELIUM® resin is one of the youngest members of organic matrices. The polymer is obtained from a low viscosity [2,3] reactive mixture of polymer solution of (meth)acrylic monomers (MMA, Alkyl acrylic) and acrylic copolymer chains (viscosity of 100 cPs) and possibly other comonomers [4]. Its polymerization is activated by a ketone peroxide as thermal initiator and can be achieved at room temperature with the presence of an iron salt-based catalyst [2]. The final material has thus two advantages: both fastness and simplicity of radical polymerization (comparable for example to unsaturated polyesters) together with the toughness of acrylic copolymer such as poly(methyl methacrylate (PMMA) where a sub-glassy mobility [5] allows a better toughness than in other composite matrices (vinylesters, unsaturated polyesters or epoxies [6] for example) .

The last open issue is the long-term stability of ELIUM® resin. Apart papers dealing with water ageing [7,8,9], the thermal ageing

case remains open to the best of our knowledge. Given the structural commonality with Polymethylmethacrylate (PMMA), thermal degradation is expected to induce both random chain scissions together with chain ends unzipping. However, it remains to assess the possible differences in kinetics with PMMA. Apparent degradation parameters were previously assessed for PMMA under anisothermal conditions [10,11] but it is tricky to predict the isothermal degradation of ELIUM® from those apparent kinetic parameters established from very high degradation temperature. Moreover, the predicting lifetime requires to understand the macromolecular changes induced by ageing [12].

That is the reason why we decided in this paper:

- to focus on isothermal degradation first under nitrogen and then in presence of oxygen,
- to perform isothermal degradation only,
- to propose a kinetic model running for degradation under air and under nitrogen basing on the elementary steps of degradation.

2. Experimental

2.1. Materials

Two kinds of ELIUM® resins (ELIUM® V1 and V2) were studied. Their approximate structure is depicted in Fig. 1. ELIUM® V2 differs from ELIUM® V1 by the addition of a divinyl groups working as a crosslinker and methacrylic acid used for improving ther-

* Corresponding author.
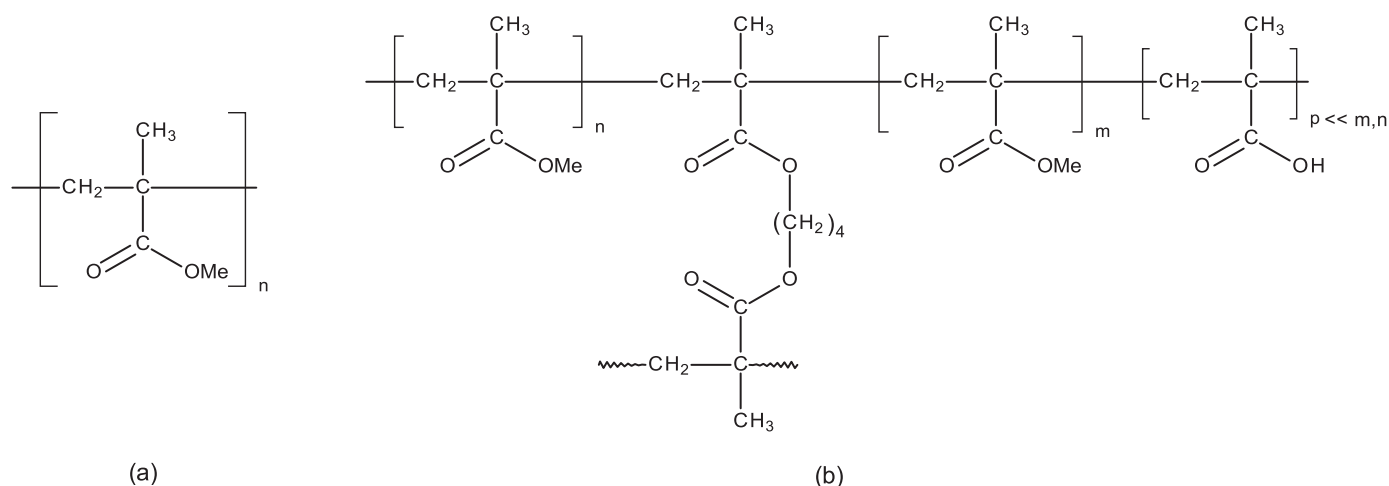*E-mail address:* emmanuel.richaud@ensam.eu (E. Richaud).

Fig. 1. Schematized structure of ELIUM V1 (a) and V2 (b).

mal stability. In other words, ELIUM V1 is a "thermoplastic resin" whereas ELIUM® V2 is processed in liquid state but gives a thermoset network after curing. ELIUM® V1 was supplied as films of about 100 μm thickness. ELIUM® V2 was supplied as 4 mm plates and about 50 μm films were samples using a Leica microtome.

A PMMA commercial grade (VM100, also supplied by Arkema) was used as a "model system". About 350 μm thickness films were prepared by compression molding using a Gibitre press by heating for 3 minutes at 200°C under 220 bars and using wedges to get right thickness.

2.2. Ageing condition

Samples were isothermally aged in thermal analysis cells of TGA device (see after) under either pure nitrogen or pure oxygen supplied by a 50 ml min^{-1} gas flow.

Some complementary tests were performed in ventilated ovens at 150, 180 and 200°C (supplied by SCS) on ELIUM V2 plates to check the thickness of oxidized layer (TOL).

2.3. Characterization

2.3.1. Thermogravimetric measurements (TGA)
TGA measurements were performed using a Q500 apparatus driven by QSeries Explorer (TA Instruments). Isothermal measurements were performed either under 100% N$_2$ or 100% O$_2$ atmosphere supplied by a continuous 50 ml min^{-1} gas flow. Isothermal degradation was performed at a constant temperature ranging from 230 to 310°C.

2.3.2. Differential Scanning Calorimetry measurements (DSC)
DSC measurements were performed using DSC Q10 apparatus (TA instruments) using the following procedure: samples were first isothermally degraded in situ either under 100% N$_2$ or 100% O$_2$ atmosphere. After cooling to 40°C, they were heated at a 10°C min^{-1} so as to determine the glass transition temperature (T$_g$) value.

2.3.3. Gel Permeation Chromatography measurements (GPC)
GPC measurements were performed on a WATERS 717+ Autosampler Instrument in THF (1 ml min^{-1}) equipped with a Waters 2414 Refractive Index detector on samples previously in situ aged in TGA cell (see above). Average molar masses are given in polystyrene equivalent.

2.3.4. Optical microscopy
Optical microscopy was used for measuring the Thickness of Oxidized Layer (TOL) for aged bulky samples. After polishing the samples to get a smooth surface, a ZEISS Axio Imager A2M optical microscope was used to obtain the TOL ((Thickness of Oxidized Layers) values.

3. Results

3.1. Stability under N$_2$

Mass loss on PMMA, ELIUM® V1 and V2 were monitored isothermally at different temperatures (from 230 to 310°C) versus time exposure under 100% N$_2$ atmosphere in TGA cell (NB: for PMMA, some experiments were done in duplicate and triplicate for checking the repeatability). Results are presented in Fig. 2.

They call for the following comments:

① at very low exposure times, a very fast decrease is observed with an initial mass loss close to 10%. In ELIUM®, it seems that the initial part is mainly due to residual monomers. The residual mass was expressed as:

$$\frac{m}{m_0} = \frac{m_v + m_p}{m_{v_0} + m_{p_0}} \tag{1}$$

Where m_v is the masse of residual (non polymerized) monomers, m_p of the volatile compounds released due to polymer decomposition. As depicted in Appendix 1 (Fig. 10) and discussed later, m_p decreases following an apparent first order kinetics, and it seems reasonable to assume that it is also the case for m_v. If so:

$$\frac{m}{m_0} = \frac{m_{v_0}.\exp(-k_v.t) + m_{p_0}.\exp(-k_{obs}.t)}{m_{v_0} + m_{p_0}} \tag{2}$$

with $k_v \gg k_{obs}$ so that at early times:

$$\frac{d}{dt}\left(\frac{m}{m_0}\right) \sim \frac{-k_v.m_{v_0}}{m_{v_0} + m_{p_0}} \tag{3}$$

Whereas, at longer times, with $m_p \gg m_v$:

$$ln\left(\frac{m}{m_0}\right) \sim \exp(-k_{obs}.t) \tag{4}$$

Both equations will be used to extract apparent rate constants of degradation. k_v was shown to be hardly temperature dependent but this is not surprising since the loss of residual monomers occurs meanwhile the cell temperature is equilibrating to the ageing temperature.

② in a second stage, mass decreases with an auto slowed down kinetics. A pseudo first order kinetics is observed for PMMA and
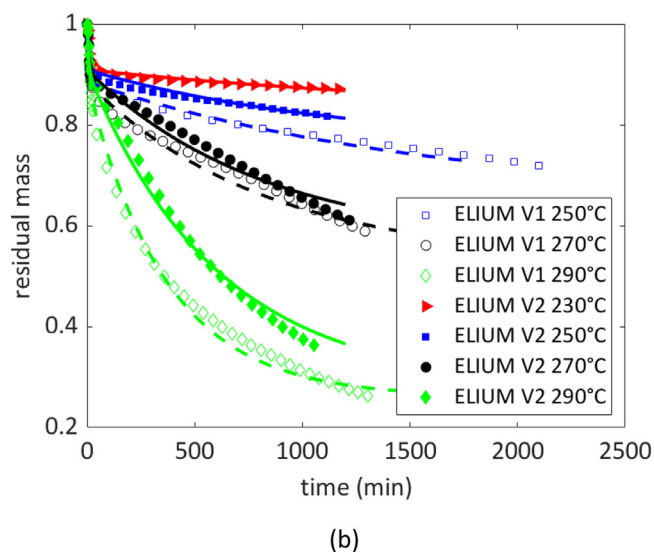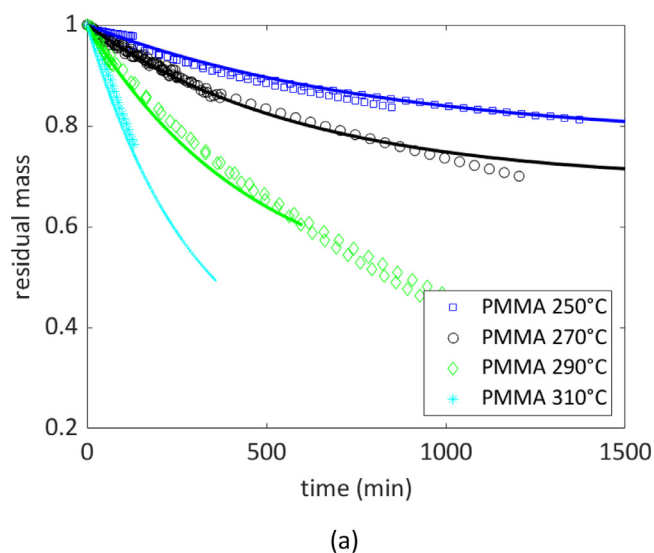
(a)

(b)

Fig. 2. Kinetics of mass changes for PMMA (a) and ELIUM® V1 and V2 (b) under N$_2$ at different temperatures. For Figs. 1a and 1b, dashed lines correspond to best kinetic model with rate constants given in Table 3 (see "Discussion"). NB: the number of experimental points is lowered for better clarity.

Fig. 3. DSC traces of unaged and ELIUM® and PMMA aged 2 h under N$_2$ at 250°C.

(a)

(b)
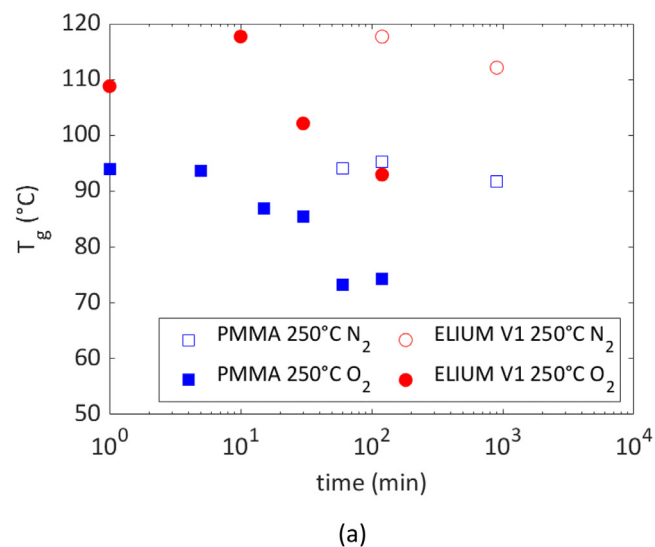
Fig. 4. T$_g$ changes of PMMA and ELIUM® V1 versus exposure time at 250°C under N$_2$ (a) and as a function of temperature for different exposure times under N$_2$ (b).

fits acceptably in a first approach for ELIUM® in the medium conversion degrees (up to almost 50% mass loss).

③ in a first approach, PMMA and ELIUM® display some comparable trends: for example, at 250°C, about 20% of the initial mass is lost after 20 h aging under 100% N$_2$ for both materials. At 270°C and 290°C, the mass loss after 20 h is in both cases close to 40% and 65%. More in detail, ® V2 which is more stable than ELIUM® V1 possibly in link with the presence of some comonomers, which will be depicted in terms of rate constants for depolymerization in the following.

To better understand the mechanisms responsible for mass loss, DSC measurements were performed in order to measure the change in glass transition value and investigate the architecture of degraded materials. Fig. 3 depicts thermograms of virgin and aged PMMA and ELIUM® V1 resin having undergone a thermal exposure in situ under nitrogen. Corresponding T$_g$ changes are given in Fig. 4a together with values for samples degraded in presence of oxygen. Under nitrogen, the glass transition temperature remains almost constant within the experimental uncertainties (contrarily to ageing oxygen, as it will be seen later). A small increase
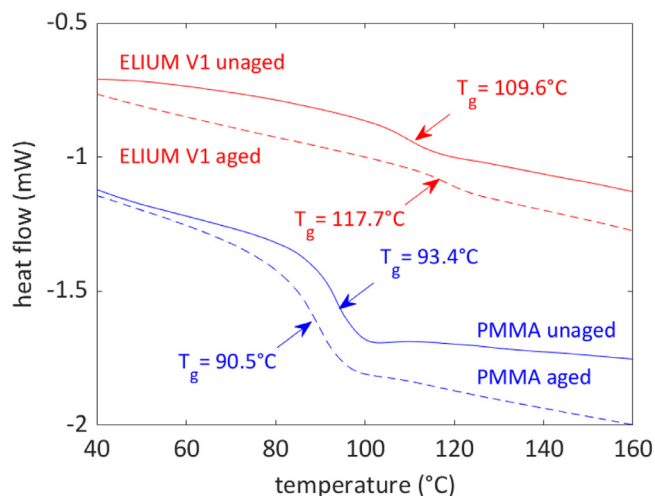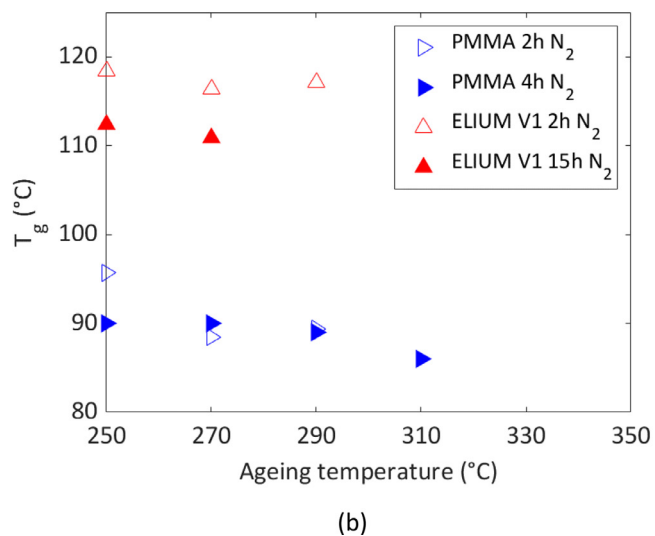
Fig. 5. GPC measurements for PMMA samples aged under N_2 or O_2 at different temperatures.

Table 1
Measured molar mass after ageing at different temperatures under 100% N_2 or 100% O_2 atmosphere.

Ageing conditions	M_w (kg mol$^{(1)}$)	M_n (kg mol^{-1})
0 h (not aged)	123.7	60.6
2h - 250°C - N_2	125.3	64.7
2h - 270°C - N_2	124.2	67.1
2h - 290°C - N_2	108.2	51.5
2h - 310°C - N_2	68.9	28.8
1h - 250°C - O_2	57	8.6
2h - 250°C - O_2	13.3	2.6
15 h - 250°C - O_2	2.1	1.3

Table 2
Measured TOL on ELIUM® V2 samples (up to 3 months aging for the highest values).

Temperature (°C)	150°C	160°C	180°C	200°C
TOL (µm)	1100-1300	1100-1200	760-870	550-830

can even be observed, maybe due to the evaporation of residual monomers (see above). This observation seems also to be true at temperatures higher than 250°C (i.e. 270 and 290°C) for different exposure times. One sees that despite significant mass loss levels (up to 30% at 290°C after 4 h exposure), T_g depletion remains relatively low (about 5°C). As it will be seen later, this is in line with the existence of a predominant unzipping mechanism i.e. a chain ends depolymerization.

Contrarily to ELIUM® V2 which is a thermoset resin i.e. insoluble, PMMA can be easily analyzed by GPC as illustrated in Fig. 5 for PMMA aged at 250, 270 and 290°C during 2 h. The measured molar masses for samples aged at 250, 270 and 290°C under N_2 for 2h are given in the Table 1. They confirm that decrease in molar mass is low which suggests that volatile segments come for the chain ends as is will be tentatively justified later.

3.2. Investigation of the stability under oxygen

The stability of samples under oxygen was first investigated by determining the thickness of oxidized layer at several temperatures (Fig. 6) for 4 mm thick plates aged in ovens under air. This latter was estimated as the total thickness of the dark edge of samples by optical microscopy. For summarizing:
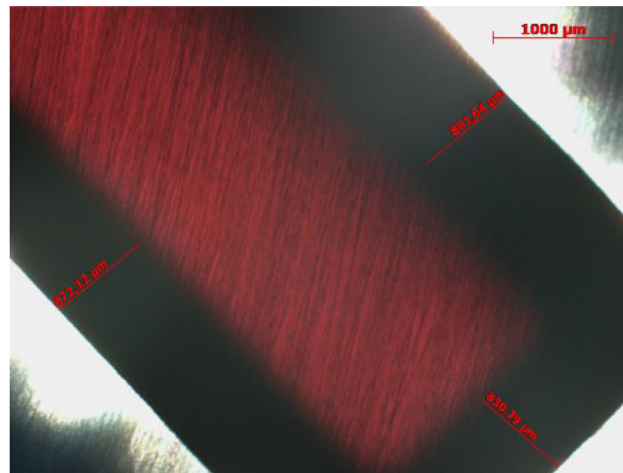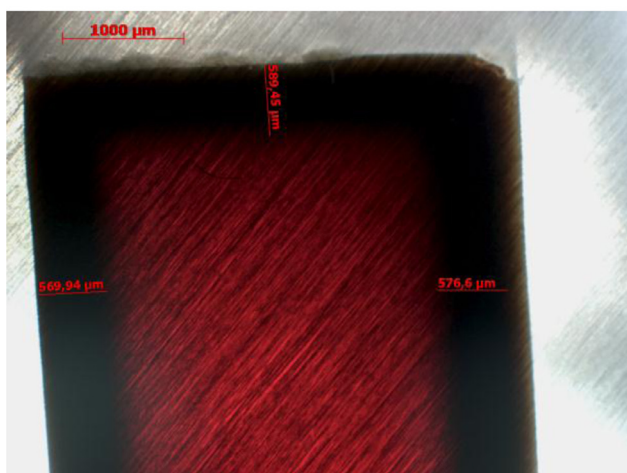
- There is no evidence of cracks occurring within the oxidized layer and favoring the propagation of this latter towards deeper layers [13]. The measured Thicknesses of Oxidized Layers (TOL) are given in Table 2.
- TOL takes an almost constant value depending only on temperature and certainly external oxygen concentration. Despite lower than in recently developed thermoset matrices (~ 1500-2000 µm in epoxidized linseed oil thermosets [14]), its value is clearly higher than in other thermosets (for instance less than 300 µm for vinyl esters, 600 µm in unsaturated polyesters [15]) degraded in comparable conditions.
- As previously described in literature [16], TOL decreases when increasing temperature.

Those values were tentatively extrapolated at temperatures under investigation (250-290°C) using Arrhenius equation. One sees that oxidation would hardly be controlled by oxygen diffusion for samples below 300 µm at 290°C so that in the following, investigations will be performed on 50 µm thin ELIUM® V2 obtained by microtomy, 150 µm ELIUM® V1 films obtained by casting reactive mixture between two plates, and 350 µm PMMA films obtained by compression molding. Moreover, the control of oxygen diffusion has only a low impact on the main conclusions of this paper.

The effect of oxygen on thermal ageing was thus investigated for example by performing isothermal TGA under pure oxygen. They are directly compared with TGA under nitrogen at the same
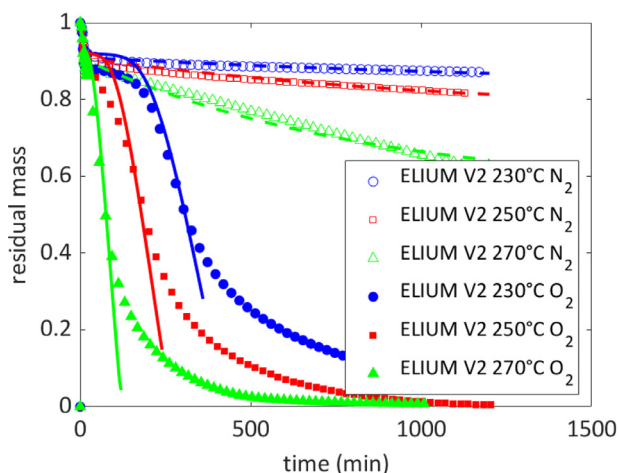

Fig. 6. Optical microscopy images of the oxidized layer at (a) 200°C 3 weeks and (b) 180°C 15 weeks (b) for ELIUM® V2 samples.

Fig. 7. Comparison of mass loss monitored by TGA under nitrogen and oxygen for 50 μm ELIUM® V2 films at several temperatures. Full and dashed lines correspond to kinetic modeling respectively under oxygen and nitrogen with rate constants given in Table 3.

Fig. 8. T_g changes vs mass loss for ELIUM® V1 resin aged under nitrogen and oxygen.

temperatures in Fig. 7. According to a preliminary interpretation, it seems that the presence of oxygen induces an auto-accelerated mass loss mechanism but in the earlier exposure time, the "pure" thermal mechanism is prominent.

Those experiments were completed by measuring the T_g changes (related to polymer backbone modifications) after isothermal ageing runs. Corresponding results are given in Fig. 4. Both PMMA and ELIUM® V1 present a strong T_g changes in those conditions (about 20°C decrease after 2 h aging). This confirms the instability of acrylic resins at high temperatures under O_2. Those strong T_g changes indicate the presence of chain scissions randomly located in PMMA, and presumably in ELIUM as well. Those latter are confirmed by GPC measurements (Fig. 5) leading to the molar mass values for samples aged at different times given in Table 2.

Last, two GC-MS analyses (subcontracted in 2MATECH, Aubière, France) were performed on gaseous compounds evolved by samples aged 1h at 250°C either under N2 or air in hermetic vials. In both cases, MMA was found to be the predominant volatile compounds (Fig. 10).

4. Discussion

The aims of this section are:

- to compare the nature of the mechanism under nitrogen and in presence of oxygen,
- to propose a kinetic modeling working for ELIUM® V1, ELIUM® V2 and PMMA with parameters related to the thermal stability,
- to adapt this kinetic model for ageing either under inert atmosphere or in presence of oxygen.

4.1. Nature of the mechanisms involved under inert atmosphere or in presence of oxygen

The most striking facts are that under oxygen, average molar mass decreases fast in conjunction with a higher level of mass loss whereas values expressing the macromolecular architecture (M_n, T_g) remains almost constant for ageing under inert atmosphere despite the occurrence of mass loss (Fig. 8).

Interestingly, for a given mass loss level, the corresponding decrease of glass transition is higher for ageing in presence of oxygen than for ageing under inert atmosphere. For discussing this result,
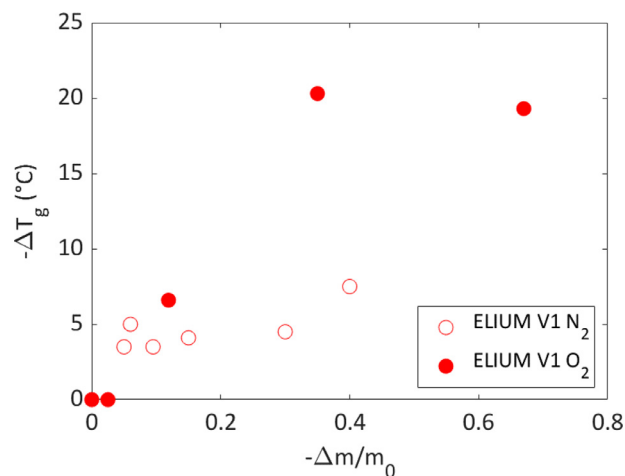
let us recall that glass transition changes with molar mass as follows [17]:

$$T_g = T_{g\infty} - k_{FF}/M_N \qquad (5)$$

Where $T_{g\infty}$ is the "fictive" value for a PMMA sample with an infinite molar mass, and k_{FF} is the Fox Flory constant (114°C and 200 K kg mol^{-1} values for PMMA are given in [18]).

M_n changes with the concentration in chain scissions:
- For random chain scissions [19]

$$\frac{1}{M_N} - \frac{1}{M_{N0}} = s \qquad (6)$$

- For chain end scissions (unzipping)

$$M_N = M_{N0} - s.M_N.M_0 \qquad (7)$$

(where M_0 is the molar mass of the monomer unit).
It comes:
- For chain ends scissions

$$T_g - T_{g0} = -\frac{k_{FF}.M_0}{M_{N0}} \cdot \frac{s}{1 - s.M_0} \qquad (8)$$

i.e. at low conversion degrees

$$dT_g/ds = -k_{FF}.M_0/M_{N0} \qquad (9)$$

- For random chain scissions

$$T_g - T_{g0} = k_{FF}.s \qquad (10)$$

i.e. at low conversion degrees

$$dT_g/ds = -k_{FF} \qquad (11)$$

Since $M_0 << M_{N0}$, it means that a limited number of chain scission has a strong effect on molar mass for random chain scissions compared to chain end scissions.

According to literature, there are three main mechanisms at the origin of unzipping (Scheme 1): random chain scissions [20] followed by the ejection of monomers located at chain ends (Scheme 1a).

- scissions located on weak sites such as head to head moieties (possibly in the middle of chains – Scheme 1b). In principle, this reaction occurs even at low temperature (around 200°C) [21].
- unzipping occurring directly at chain ends holding double bonds [22] (Scheme 1c and 1d), those latter being expected since no transfer agent was used for ELIUM® manufacturing.
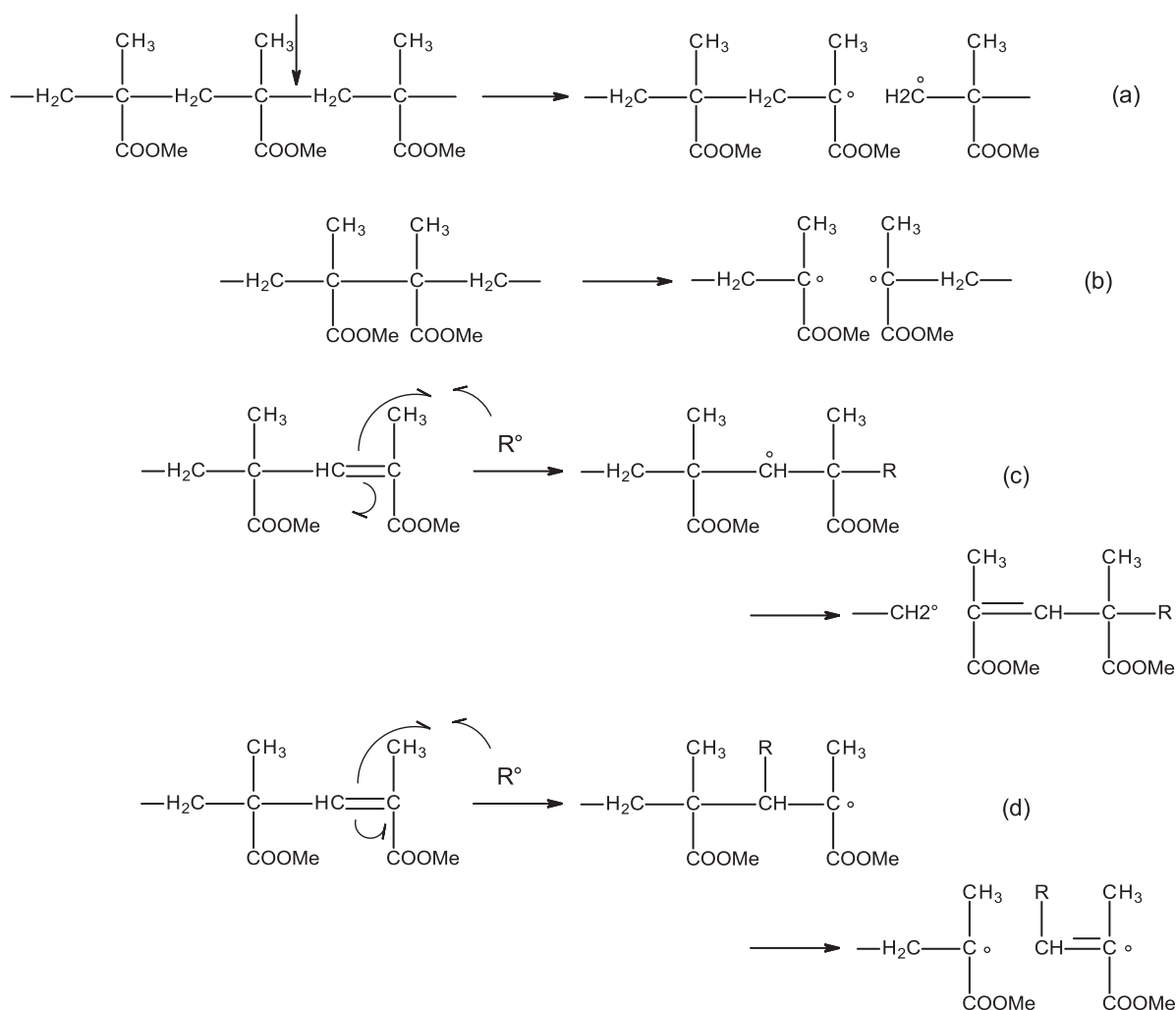
Scheme 1. Initiation mechanism of thermal degradation.

According to the glass transition and molar mass changes (see previous section), we assumed that unzipping occurs mainly at the chain ends, consistently with other results [20]. In other words, it seems to us that: under inert atmosphere, the mechanism is an unzipping mechanism occurring by chain ends, consistently with literature data [23].

- under oxygen, the unzipping mechanism is complicated by the fact that alkyl radicals can simultaneously undergo unzipping and react with oxygen and induce a degradation mechanism where chain scissions can occur simultaneously on the polymer chain.

4.2. Degradation mechanism under inert atmosphere

According to many previous researches, it can be considered that the auto-decelerated shape of mass loss curves for PMMA [21,24] based polymers obeys a first order kinetics:

$$\frac{dm}{dt} = - k_{obs} \cdot m \tag{12}$$

Observed apparent rate constants (k_{obs}) can be assessed from first order diagrams (see Fig. 2). Corresponding values are plotted in Fig. 9 together with values for PMMA either from this work or from literature [21,24].

In a first approach, data measured in this work in the same temperature range for PMMA, ELIUM® V1 and ELIUM® V2 are relatively comparable. They reasonably fit with the Arrhenius law, with apparent activation energy equal to 113.5 kJ mol^{-1} (PMMA studied in this work) or ~ 140 kJ mol^{-1} for ELIUM® V1 and ELIUM® V2. Reversely, data from [21,24] seem responsible for a certain distortion in the Arrhenius diagram with a higher activation energy (~ 200 kJ mol^{-1}). This curvature can be explained as follows: at higher temperature, initiation results either from chain end or random chain scission (whereas only the first one exists at temperatures below 300°C). As it will be seen later, since the apparent rate constant for depolymerization is a function of rate constant for elementary steps (Eq. 19), the existence of those two competing mechanisms can result in a curvature in Arrhenius diagram [25,26].

According to those data, ELIUM® V2 resin seems slightly more stable than ELIUM® V1 towards the unzipping degradation, which can be explained as follows: ELIUM® V2 reactive mixture contains a slight percentage of 1,4 butanediol dimethacrylate and methacrylic acid working which may act as depolymerization inhibitors (the effect of ethylene glygol dimethacylte is illustrated in [27]).

The "first order" plot (Fig. 2) and the apparent rate constant allow easily to screen and characterize the stability of acrylic resins. However, it remains quite empirical since it does not really take
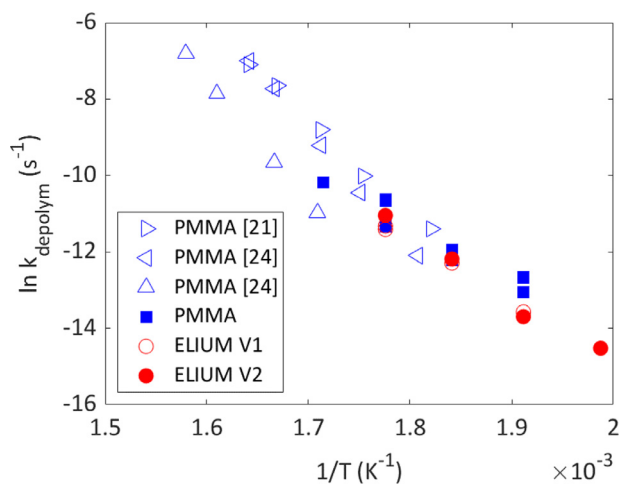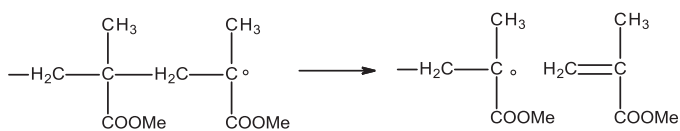
Fig. 9. Arrhenius diagram for apparent rate constants of thermal decomposition under nitrogen atmosphere.
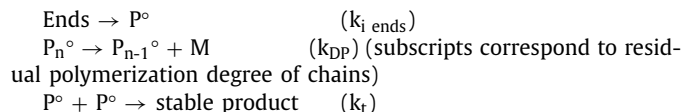

Scheme 2. Depropagation for unzipping.

into account the chemical mechanisms at the origin of mass loss (as it will be seen later, this is needed to predict the degradation under air). A more complete (but simplified) mechanism is summarized here below:

① As discussed above, initiation would start by chain ends.

② Depropagation (« unzipping ») leads to monomer release (Scheme 2).

③ Last, termination corresponds to the reaction between two radicals to form a "stable" chain (Scheme 3). It can involve sec-

ondary and tertiary radicals (Scheme 1a-1d). The coupling of tertiary radicals (Scheme 1d) creates an unstable head to head group likely to initiate further degradation. In a first approach, this latter reaction was neglected compared to the other reactions [28,29] so that we do not have to add a new initiation reaction (with a supplementary kinetic parameter) in the model.

Assuming a bimolecular termination process, this derived kinetic model is thus:

$$\text{Ends} \rightarrow P^{\circ} \qquad (k_{i\ ends})$$
$$P_n^{\circ} \rightarrow P_{n-1}^{\circ} + M \qquad (k_{DP}) \text{ (subscripts correspond to residual polymerization degree of chains)}$$
$$P^{\circ} + P^{\circ} \rightarrow \text{stable product} \qquad (k_t)$$

In this last case, it can for example be shown:

$$\frac{d[P^{\circ}]}{dt} = k_{i\ ends}[ends] - 2k_t[P^{\circ}]^2 \qquad (13)$$

[ends] is the concentration in chain ends likely to initiate depolymerization (vinyl groups for example). For PMMA, it might be close to ρ_0/M_{n0} at t = 0 (where ρ_0 is the polymer density and M_{n0} its initial average number molar mass). Under the assumption that steady state is quickly reached, it gives:

$$[P^{\circ}] = \sqrt{\frac{1}{2k_b} \cdot \left(\frac{k_{i\ ends} \cdot \rho_0}{M_n} \right)} \qquad (14)$$

The concentration of released monomers [M] is given by:

$$\frac{d[M]}{dt} = -k_{DP}.[P^{\circ}] \qquad (15)$$

Which leads to the theoretical expression of mass loss rate for unzipping:

$$\frac{d\left(\frac{m}{m_0}\right)}{dt} = -\frac{M_m}{\rho_0} \cdot \frac{d[M]}{dt} = -\frac{M_m}{\rho_0} \cdot k_{DP} \cdot \sqrt{\frac{k_{i\ ends} \cdot \rho_0}{2k_t.M_n}} \qquad (16)$$
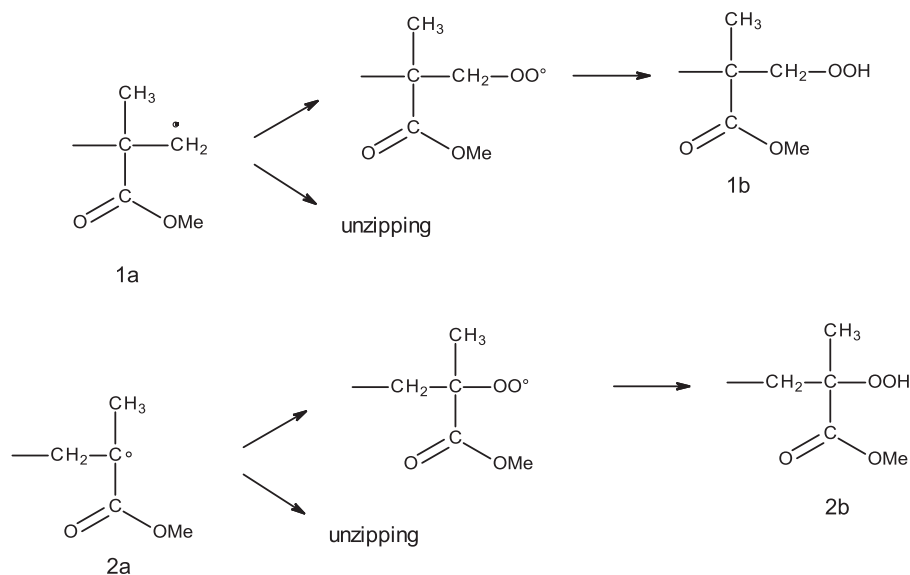
Where M_m is the mass of the monomer released from unzipping.

In the (empirical) first order model, one has:

$$[M] = [M]_0.\exp(-k_{obs}.t) \qquad (17)$$
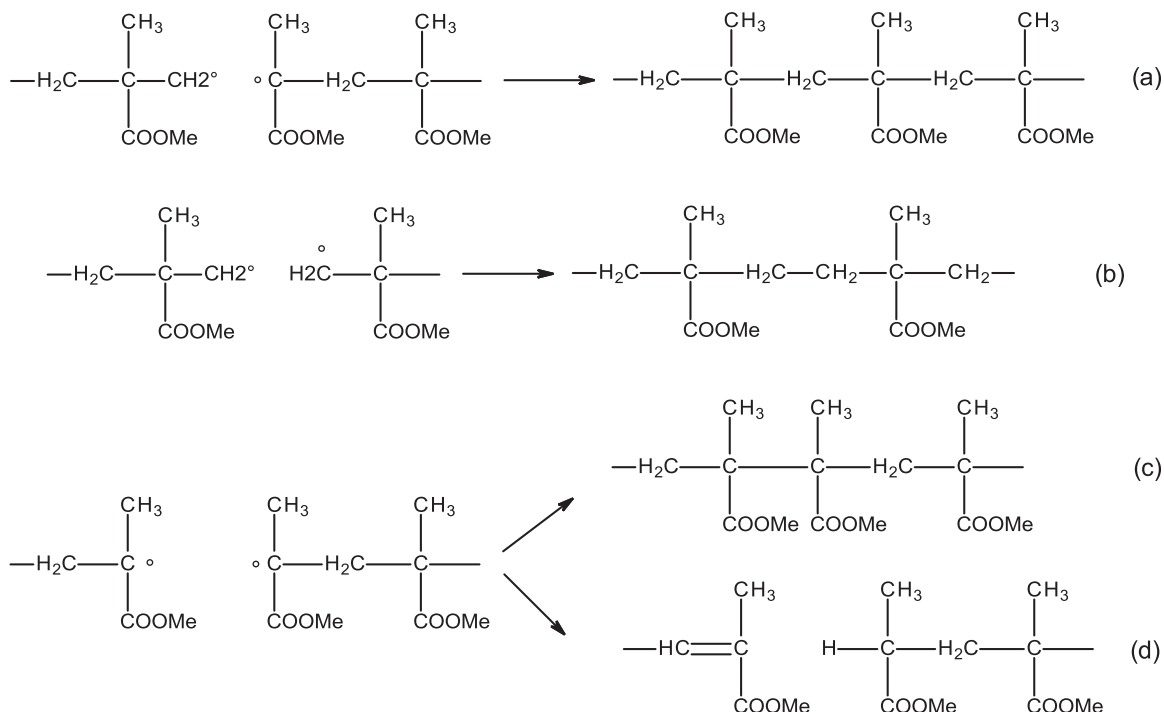
Scheme 3. Termination for unzipping.

Scheme 4. Fate of alkyl radicals under air.

i.e. at low conversion degrees:

$$[M]/[M]_0 \sim 1 - k_{obs} \cdot t \tag{18}$$

So that this kinetic model converges with the empirical first order model at steady state where the following equality is observed:

$$k_{obs} = \frac{M_m}{\rho_0} \cdot k_{DP} \cdot \sqrt{\frac{k_{i\ ends} \cdot \rho}{2 k_t \cdot M_n}} \tag{19}$$

It suggests that Eq. 19 can be used as a simplified relationship to estimate the relative orders of magnitude of k_i, k_{DP}, k_t from the apparent k_{obs} value estimated in Fig. 2.

In order to estimate all the rate constants, the differential system was solved using Scilab® software with the script given in "Supplementary Informations". The strategy is to identify rate constants from the fitting of data given in Fig. 2. In order to minimize the number of adjustable kinetic parameters, some values (k_t, $[ends]_0$) related to elementary steps were fixed as discussed below. The missing values must verify (at least roughly) Eq. 19.

In the case of radical PMMA polymerization, the rate constant between two alkyl radical ended PMMA chains is $k_t \sim 5.10^7$ l mol^{-1} s^{-1} [30]. There is no reason, for us, to consider there is any difference with PMMA.

Since PMMA and ELIUM® resins display an almost common behavior (apart the release of free monomers), we decided to consider that:

- in PMMA, the initial concentration in chain ends is ρ_0 /M_{n0} ~ 1/60 mol l^{-1}.
- in ELIUM® resin, this concentration is the same. In fact, even if this is an approximation, it can be easily verified that model simulations remain almost the same provided that the quantity k_i/M_{n0} remains constant.

Using those rules for rate constants, the rate constant for unzipping can thus be estimated. They allow to fit mass loss curves (Fig. 2) and are thus expected to express the reactivity of each system.
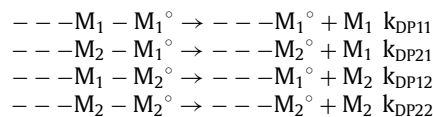
It can be verified that k_{obs} (derived from Fig. 2) and k_{obs}^* (derived from Eq. 19) are relatively close. In other words, despite some approximations made for the concentration of radicals in steady state, it validates the proposed kinetic model. k_{DP} is found to verify Arrhenius law with an activation energy E_{aDP} ~ 100 kJ mol^{-1},

which can be discussed as follows: for propagation reaction in PMMA polymerization, the activation energy (E_{aP}) is reported to be about 25 kJ mol^{-1} [31] meanwhile the reaction enthalpy for polymerization reaction is ΔH_r ~ -60 kJ mol^{-1} [32]. It is hence not surprising to observe $E_{aDP} \sim E_{aP} - \Delta H_r$.

According to [33], the rate of scission of chain ends for a PMMA synthesized by Reversible Addition Fragmentation chain Transfer (k_i) is given by $1.06 \times 10^6 \times$ exp(-77600/RT) s^{-1}. In a certain way, it could be considered that RAFT agents are chosen so as to make possible the "reactivation" of PMMA chain [23] end into radical living forms so that k_i is expected here to be lower, in good agreement with the values we used for our model. Reversely, the activation energy of initiation reaction is found lower than in ref [24] (more than 200 kJ mol^{-1}) where unzipping is studied at high temperature where random chain scission might be the main initiation mode.

Since k_i is in part unknown, this investigation was completed by a parametric study (see "Supplementary Informations" file). For summarizing, there is an interplay between all rate constants so that many set could acceptably fit the experimental data. However, an accurate simulation of the curve cannot be obtained if one significant error (for example a factor 2 on one rate constant) is made, because it cannot be compensated by changes on other parameters.

Interestingly, k_{DP} is found lower for example for ELUM V2 than ELIUM V1. This might be in link with the presence of comonomers working as "internal stabilizers". In the future, a more thorough description of the unzipping reaction would be based on a scheme closed to copolymerization process:

$$- - - M_1 - M_1^\circ \rightarrow - - - M_1^\circ + M_1 \quad k_{DP11}$$
$$- - - M_2 - M_1^\circ \rightarrow - - - M_2^\circ + M_1 \quad k_{DP21}$$
$$- - - M_1 - M_2^\circ \rightarrow - - - M_1^\circ + M_2 \quad k_{DP12}$$
$$- - - M_2 - M_2^\circ \rightarrow - - - M_2^\circ + M_2 \quad k_{DP22}$$

Where M_1 is MMA and M_2 a comonomer, such as typically k_{DP11} >> k_{DP12} for example.

4.3. Degradation mechanism in presence of oxygen

According to Scheme 4, two kinds of alkyl radicals can be generated during PMMA or ELIUM® thermolysis and both can react with oxygen to give a hydroperoxide.

Table 3
Kinetic parameters for degradation used for fitting mass loss curves (Figs. 2 and 7). k_{obs} comes from Fig. 2 and $k_{obs}*$ from Eq. 19.

	T (°C)	[V] (mol l⁻¹)	k_v (s⁻¹)	k_i (s⁻¹)	k_{DP} (s⁻¹)	k_t (l⁻¹ s⁻¹)	k_{obs} (s⁻¹)	$k_{obs}*$ (s⁻¹)	k_1 (s⁻¹)	k_2 (l mol⁻¹ s⁻¹)	k_3 (l mol⁻¹ s⁻¹)	k_5 (l mol⁻¹ s⁻¹)
ELIUM V2	230	1	2.3×10^{-3}	1.1×10^{-5}	110	5.0×10^7	4.9×10^{-7}	4.1×10^{-7}	7.0×10^{-4}	1.0×10^5	320	5.0×10^7
ELIUM V2	250	1	2.3×10^{-3}	2.75×10^{-5}	200		1.1×10^{-6}	1.2×10^{-6}	1.25×10^{-3}	1.0×10^5	650	5.0×10^7
ELIUM V1	250	1.5	2.3×10^{-3}	2.0×10^{-5}	375		1.3×10^{-6}	1.9×10^{-6}	-	-	-	-
PMMA	250	0	-	4.0×10^{-5}	450		2.8×10^{-6}	3.2×10^{-6}	-	-	-	-
ELIUM V2	270	1	2.3×10^{-3}	3.5×10^{-5}	550		5.1×10^{-6}	3.7×10^{-6}	3.5×10^{-3}	1.0×10^5	1225	5.0×10^7
ELIUM V1	270	1.5	2.3×10^{-3}	4.0×10^{-5}	800		4.6×10^{-6}	5.7×10^{-6}	-	-	-	-
PMMA	270	0	-	5.5×10^{-5}	720		5.7×10^{-6}	6.0×10^{-6}	-	-	-	-
ELIUM V2	290	1	2.3×10^{-3}	5.5×10^{-5}	1400		1.6×10^{-5}	1.2×10^{-5}	-	-	-	-
ELIUM V1	290	1.5	2.3×10^{-3}	9.0×10^{-5}	2100		1.2×10^{-5}	2.2×10^{-5}	-	-	-	-
PMMA	290	0	-	7.0×10^{-5}	1450		1.8×10^{-5}	1.4×10^{-5}	-	-	-	-
PMMA	310	0	-	11×10^{-5}	2400		3.8×10^{-5}	2.8×10^{-5}	-	-	-	-
E_a (kJ mol⁻¹)	**ELIUM V2**			60.1	101.4	0	140.2	-	179.6	0	76.3	0
	ELIUM V1			92.0	105.3		135.3	-	-	-	-	-
	PMMA			41.4	73.3		113.5	-	-	-	-	-

From a kinetic point of view, the rate constant for the reaction $P° + O_2 \rightarrow POO°$ (k_2) is reported to be about 10^8 l mol⁻¹ s⁻¹ [34] whereas the solubility in polymers is about 10^{-3} mol l⁻¹ [35]. The balance between the rate of oxidation and unzipping is given by $k_2[O_2]/k_{DP} \sim 10^5/k_{DP}$ and clearly exceeds 1 for all temperatures under investigation. In other words, an oxidation mechanism takes place and predominates. However, MMA is the main volatile product (like under inert atmosphere) meaning that radicals are mainly located by chain ends meanwhile random chain scission seem to co-exist with chain ends unzipping. Basing on existing literature, a speculative mechanism can be proposed (see "Appendix 2"), despite more analytical data are needed to validate it. We thus tried to model the effect of oxygen on mass loss rate by adding the mechanisms (summarized as 1, 2, 3 and 5 reactions) derived from the Basic Autooxidation Scheme to the unzipping scheme presented in the previous section. The complete scheme becomes:
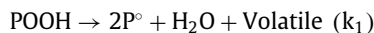
Initiation by thermolysis : Ends $\rightarrow$ P° (k_i)

Depropagation : $P_n° \rightarrow P_{n-1}° + M$ (k_{DP})

Bimolecular termination :
    P° + P° $\rightarrow$ stable product (k_t)
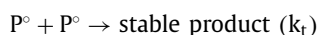
Initiation by hydroperoxides decomposition :
    POOH $\rightarrow$ 2P° + H_2O + Volatile (k_1)

Propagation : P° + O_2 $\rightarrow$ POO° (k_2)

Propagation : POO° + PH $\rightarrow$ POOH + P° (k_3)

Bimolecular termination : P° + POO° $\rightarrow$ inactive product (k_5)

Of course, this is a simplified view of the complete degradation mechanisms: or example the termination between POO° and POO° is not taken into account here. This latter actually predominates under enhanced oxygen pressures [36] which is not the case here, and adding it to the mechanistic scheme would induce a supplementary parameter to be determined.

In a first approach, it was chosen to present here the "simplest" scheme (with the advantage of a very limited number of adjustable kinetic parameters). This mechanistic scheme leads to the following differential system:

$$\frac{d[P°]}{dt} = k_i[PH] - 2k_t[P°]^2 + 2k_1[POOH] - k_2[P°][O_2] + k_3[POO°][PH] - k_5[P°][POO°] \tag{20}$$

$$\frac{d[POO°]}{dt} = k_2[P°][O_2] - k_3[POO°][PH] - k_5[P°][POO°] \tag{21}$$

$$\frac{d[POOH]}{dt} = -k_1[POOH] + k_3[POO°][PH] + k_5[POO°][P°] \tag{22}$$

We assumed here that termination between P° and POO° generates dialkylperoxides kinetically equivalent to hydroperoxides in term of decomposition.

The mass of released volatiles (i.e. reactive substrate with abstractable hydrogen to generate hydroperoxides POOH) is given by:

$$\frac{dm_p/m_{p0}}{dt} = -\frac{M_0}{\rho}(k_i[PH] + k_{DP}[P°]) + \frac{32}{\rho}k_2[P°][O_2] - \frac{18 + M_1}{\rho}k_1[POOH] \tag{23}$$

And for unpolymerized volatiles groups:

$$\frac{dm_v/m_{v0}}{dt} = -\frac{M_0}{\rho}(k_{vap}[V]) \tag{24}$$

M_0 is the molar mass of a monomer unit released from unzipping reaction (100 g mol⁻¹). M_1 is the molar mass of a volatile compound ejected from the decomposition of alkoxy. This is an adjustable parameter since many kinds of volatiles are released (see for example Scheme 5). The overall mass changes are thus given by:

$$\frac{dm}{dt} = \frac{m_{v0} \times \frac{dm_v/m_{v0}}{dt} + m_{p0} \times \frac{dm_p/m_{20}}{dt}}{m_{v0} + m_{p0}} \tag{25}$$

The corresponding script is given in Supplementary Information file. To simulate the experimental results, it remains now to assess the kinetic parameters as explained below:

① The oxygen concentration is on the order of $[O_2] = 10^{-4}$ l l⁻¹ mmHg⁻¹ = 0.003 mol l⁻¹ [35].

② k_3 (for the POO° + PH $\rightarrow$ POOH + P°) propagation reaction corresponds to a mechanism involving chain methylene predominates. Using the relation reported by Korcek [37]:

$$\log k_3(30°C) = 16.4 - 0.0477 \cdot BDE \tag{26}$$

$$E_3 = 0.55 \cdot (BDE - 261.5) \tag{27}$$

k_3 and E_3 were calculated using BDE = 395 kJ mol⁻¹ (i.e. a value close to the case of methylenic groups in PE). Interestingly, $E_3 < E_{aDP}$ which means that unzipping is favored at high temperature

whereas oxidation would predominate at lower temperatures and possibly in use conditions.

③ According to [38], the reactivity of alkyl is very high which justifies that $k_{t\,(P° + P°)} \sim k_{5\,(P° + POO°)}$ with an activation energy close to 0.

Finally, three adjustable parameters remain:

- k_1 expresses the (un)stability of hydroperoxides. This value is not, to our knowledge, documented in PMMA. Its value is directly linked to the length of the "induction period" for mass loss (see Fig. 6).
- k_2 is usually reported to be about 10^8 l mol^{-1} s^{-1}, and it is usually observed $k_2 \sim k_5$. Its value is not observed to be temperature dependent. Here, k_2 was adjusted in particular to fit the slope of the main mass loss stage under oxygen. Its value was found lower but this difference can originate from the simplifications in the mechanistic scheme.
- M_1 value also triggers the shape of mass loss curve after induction period. On one side, the molar mass of volatiles is low for compounds envisaged in the mechanism given in Appendix 2 (69 g mol^{-1} for formaldehyde + carbon dioxide, 102 g mol^{-1} for methyl pyruvate), but on the other side, chain scissions occurring on two close units can generate bigger volatile species. Here, M_1 was arbitrarily fixed equal to 85 g mol^{-1} but it is clear that a more thorough identification of volatiles are needed.

The final set of rate constants permitting a fair fitting of degradation under oxygen starting from the degradation model under oxygen is given in Table 3. We emphasize that a deeper insight in the understanding of the mechanism is required to justify those rate constants in terms of structure-properties relationships.

5. Conclusions

This paper investigates the thermal degradation under nitrogen or in presence of oxygen of ELIUM® resins, together with PMMA chosen as a model system. Degradation was monitored in situ by TGA (mass loss), together with a study of macromolecular architecture by T_g measurements using DSC and molar mass measurement by GPC. Experimental data showed that thermal degradation under nitrogen displayed two significant features: it is auto-decelerated with minor changes on polymer skeleton whereas degradation in presence of oxygen displays an auto-acceleration and strong macromolecular changes. It led us to a first kinetic model derived from the mechanistic scheme for unzipping (depolymerization) under inert atmosphere with supplementary reaction derived from the basic autoxidation scheme under oxygen. Despite the use of a limited number of adjustable parameters, reasonable simulations can be obtained at least for the moderate conversion degrees (up to 50% mass loss) with kinetic parameters being almost the same for PMMA and ELIUM® resins. The next step would be to better precise for example the depropagation step in the case of ELIUM® resins which are very often copolymers so that depropagation step is actually comparable to the scheme established for co-oxidation or copolymerization.

Declaration of Competing Interest

We hereby confirm that we have no conflict of interest with the paper

Supplementary materials

Supplementary material associated with this article can be found, in the online version, at doi:10.1016/j.polymdegradstab.2021.109523.
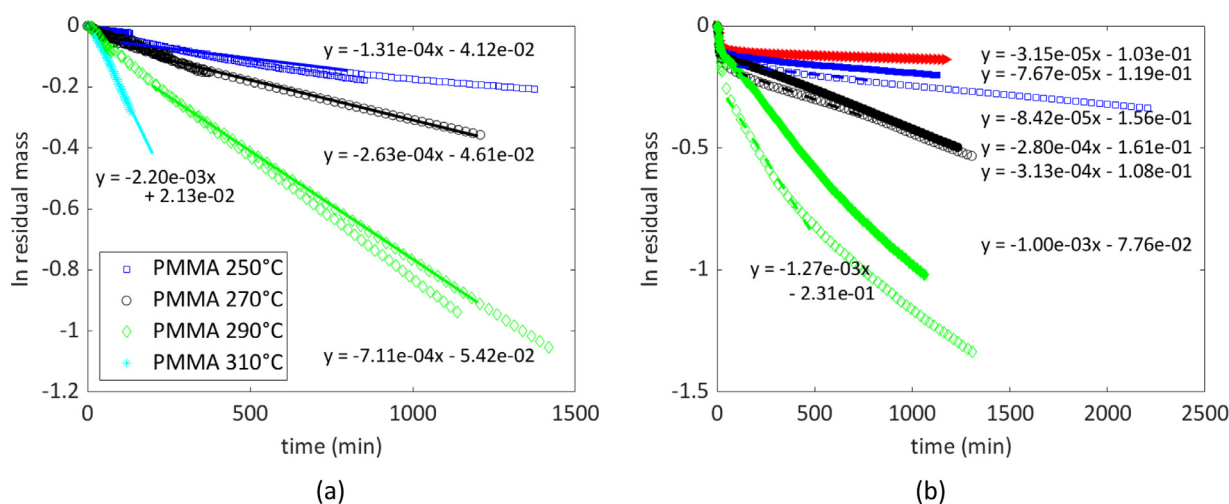
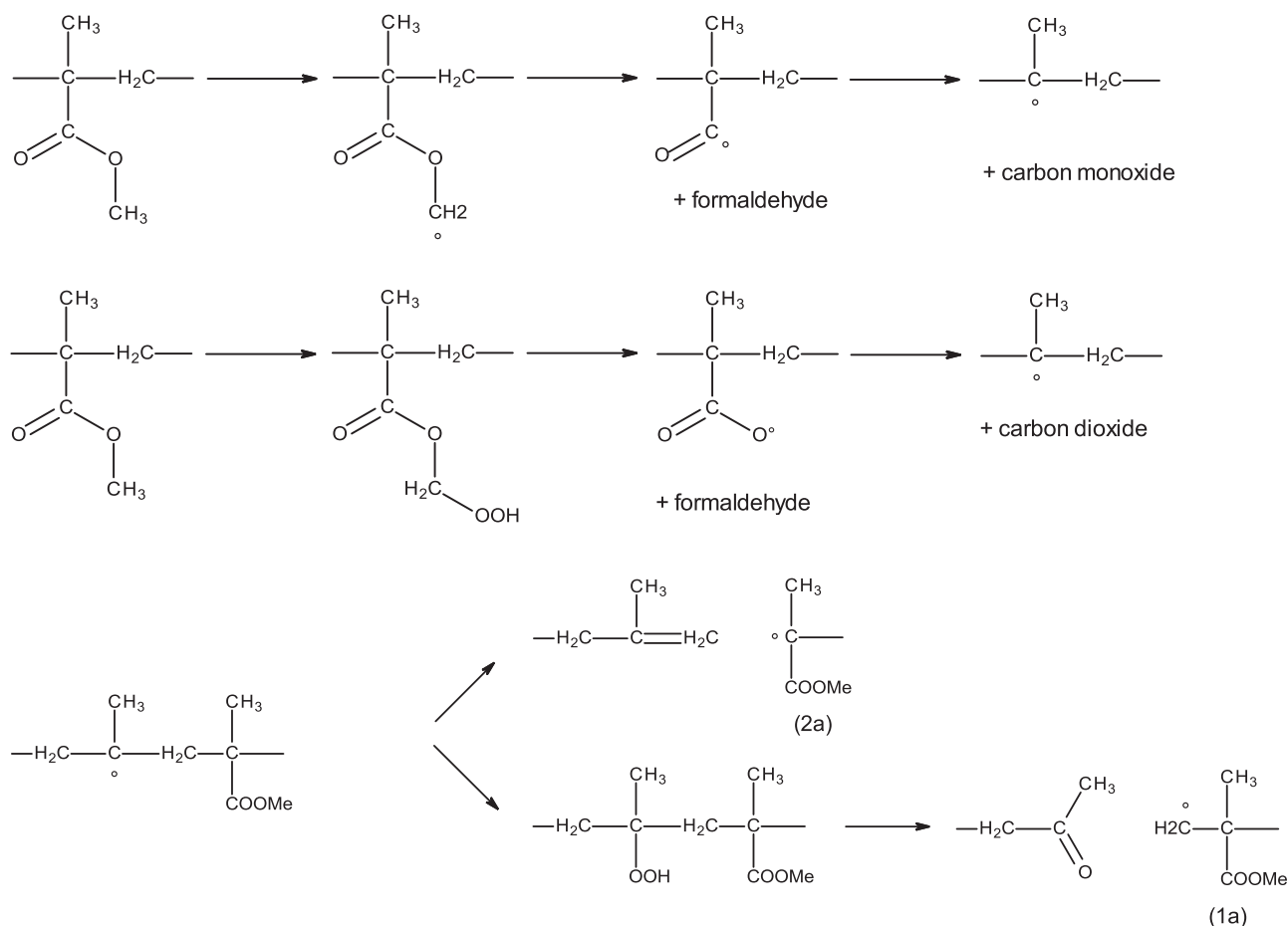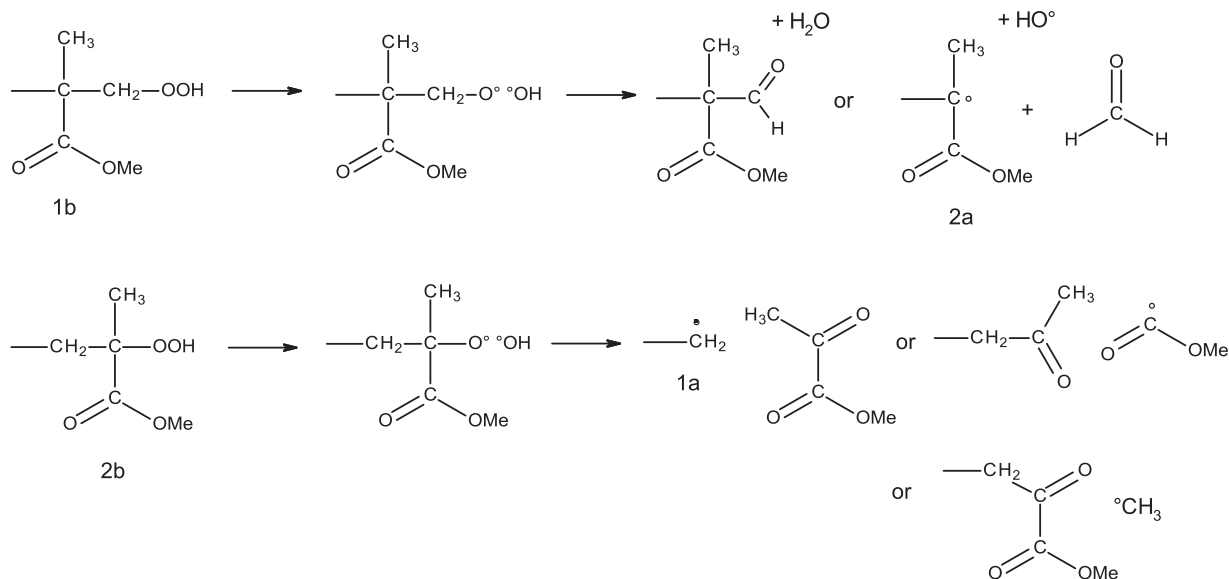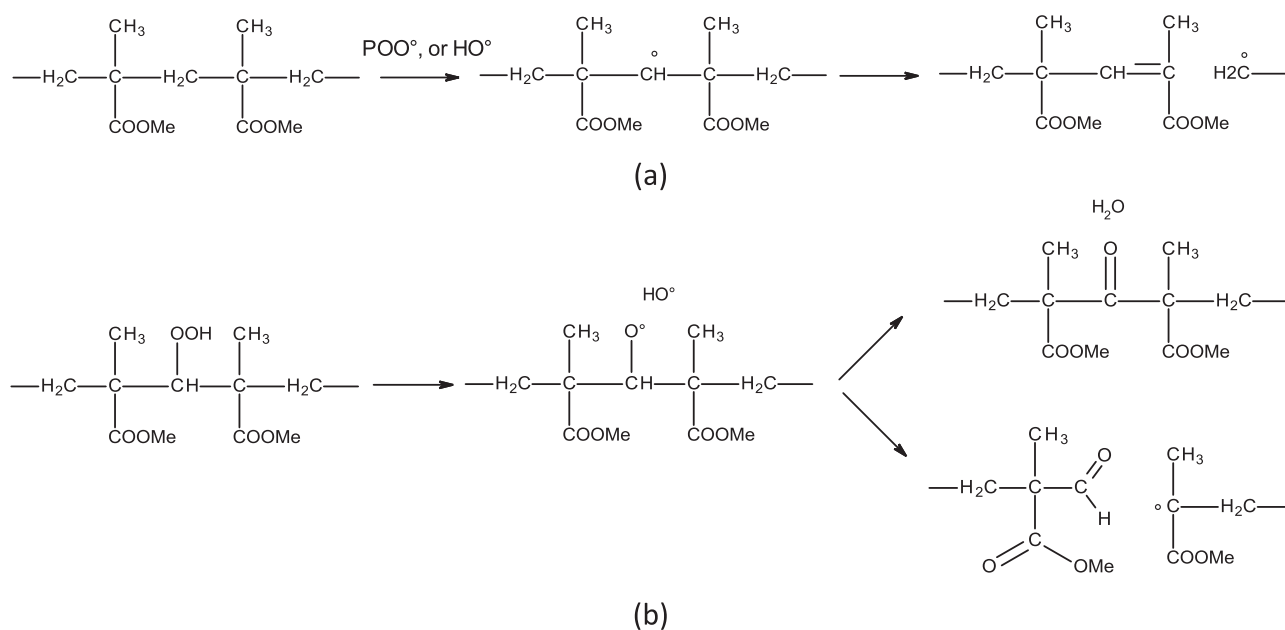## Appendix 1. First order diagrams for mass loss curves

Fig. 10. First order diagrams for kinetics of mass changes for PMMA (a) and ELIUM® V1 and V2 (b) under N_2 at different temperatures. The slopes are related to the first order mass loss equation (see "Discussion") and are given in Table 3 as k_{obs}.

Appendix 2. Proposal of a degradation mechanism

According to Scheme 4, two kinds of alkyl are formed and lead to at least two kinds of hydroperoxides, the possible decomposition products of which being given in Scheme 5:

However, one sees that such a mechanism only converts 1a alkyl radicals into 2a ones, and 2a into 1a, i.e. that reactive species remain located on chain ends. It does not explain why molar mass of PMMA chain decrease very fast (see our results in "4.1. Nature of the mechanisms involved under inert atmosphere or in presence of

Scheme 5. Decomposition of hydroperoxides in PMMA and ELIUM® resin.

Scheme 6. Oxidation mechanism involving methyl ester group.

(a)

(b)

Scheme 7. Oxidation mechanism involving the methylene group.

oxygen" or in ref [39]) and the faster degradation (Fig. 6) observed under oxygen compared to under nitrogen.

Another mechanism can be envisaged. It is based on the radical of CH groups hold by repetitive units randomly located in the polymer chains for example by many kinds of radicals (for example HO°, or peroxy radicals…). Three reactive groups can be envisaged:

- methyl in α position if tertiary carbons, which should be very stable,
- methylene –CH$_2$, and methyl groups in α position of ester, which are expected to be more reactive.

It is difficult at this stage to quantify the relative proportion of reactions involving C-H (2) and C-H (3) groups. Both C-H actually would display bond dissociation energy close to 390 kJ mol^{-1} [37,40]. However, at elevated temperatures such as investigated here, it seems that they can easily lead to 1a or 1b radicals. For example, after a radical attack, a –O-CH$_2$° radical would be generated (Scheme 6). Its decomposition could generate formaldehyde together with a carboxyl radical. This latter decomposes into a tertiary radical that will undergo a chain scission to regenerate 1a and 2a radicals so that the unzipping can go on. It explains why, even under air, methyl methacrylate is the major volatile product (see [36]).

If we consider now the alkyl radicals coming from the radical attack of methylenes, it seems also that they can rearrange by beta scission and give 1a radicals (Scheme 7a) [41].

In other words, the initiation reaction can be summarized as follows:

$$POOH \rightarrow PO° + HO°$$
$$HO° + R-H \rightarrow P° + H_2O$$
$$PO° \rightarrow volatile + P°$$
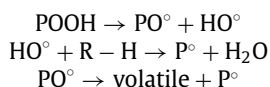
The decomposition of POOH is supposed to be the limiting step whereas the decomposition of radicals is supposed to be very fast. Finally, we have:

$$POOH \rightarrow 2P° + H_2O + volatiles$$
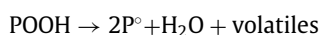
For the propagation reaction, according to Billingham [42] or Schnabel and coll [39], the reactivity of chain methylenes could prevails and induces the formation of hydroperoxides, decomposing as described in Scheme 7b. It justifies why chain scis-

sions would occur randomly (see "4.1. Nature of the mechanisms involved under inert atmosphere or in presence of oxygen"). Since each P° radical created from C-H abstraction rearrange into a "chain end radical", it can be considered that POO° + RH → POO° + P°.

Those reactions justify to implement the Basic Autoxidation Scheme (see part "4.3. Degradation mechanism in presence of oxygen").

CRediT authorship contribution statement

Mohamed Souheib Chebil: Data curtion, Formal analysis, Investigation, Writing – original draft. **Guillaume Bouaoulo:** Data curtion, Formal analysis. **Pierre Gerard:** Data curtion, Methodology, Writing – original draft. **Salma EL Euch:** Funding acquisition, Methodology, Project administration, Supervision. **Hervé Issard:** Funding acquisition, Methodology, Project administration, Supervision. **Emmanuel Richaud:** Formal analysis, Investigation, Conceptualization, Methodology, Project administration, Supervision, Writing – original draft.

References

[1] M. Arhant, P. Davies, « Marine composites - design and performance » Woodhead Publishing Series in Composites Science and Engineering, in: Chap 2 - Thermoplastic Matrix Composites For Marine Applications, 2019, pp. 31–53.

[2] S.K. Bhudolia, P. Perrotey, S.C. Joshi, Optimizing polymer infusion process for thin ply textile composites with novel matrix system, Materials 10 (2017) 293.

[3] K. van Rijswijk, H.E.N. Bersee, Review : reactive processing of textile fiber-reinforced thermoplastic composites – an overview, Composites 38 (2007) 666–681.

[4] https://patents.google.com/patent/WO2014135815A1/fr

[5] J. Sondhau, M. Lantz, B. Gotsmann, A. Schirmeisen, β-Relaxation of PMMA: tip size and stress effects in friction force microscopy, Langmuir 31 (2015) 5398–5405.

[6] W. Obande, D. Mamalis, D. Ray, L. Yang, C.M.Ó Brádaigh, Mechanical and thermomechanical characterisation of vacuum-infused thermoplastic- and thermoset-based composites, Mater. Des. 175 (2019) 107828.

[7] A. Chilali, W. Zouari, M. Assarar, H. Kebir, R. Ayad, Effect of water ageing on the load-unload cyclic behaviour of flax fibre-reinforced thermoplastic and thermosetting composites, Compos. Struct. 183 (2018) 309–319.

[8] L.C. Miranda Barbosa, M. Santos, T.L. Lara Oliveira, G. Ferreira Gomes, A.C. Ancelotti Junior, Effects of moisture absorption on mechanical and viscoelastic properties in liquid thermoplastic resin/carbon fiber composites, Polym. Eng. Sci. 59 (2019) 2185–2194.

[9] P. Davies, P.Y. Le Gac, M.Le Gall, . Influence of sea water aging on the mechanical behaviour of acrylic matrix composites, Appl. Compos. Mater. 24 (2017) 97–111.

[10] M. Ferriol, A. Gentilhomme, M. Cochez, N. Oget, J.L. Mieloszynski, Thermal degradation of poly(methyl methacrylate) (PMMA): modelling of DTG and TG curves, Polym. Degrad. Stab. 79 (2003) 271–281.

[11] Z. Gao, T. Kaneko, D. Hou, M. Nakada, Kinetics of thermal degradation of poly(methyl methacrylate) studied with the assistance of the fractional conversion at the maximum reaction rate, Polym. Degrad. Stab. 84 (2004) 399–403.

[12] P. Gilormini, E. Richaud, J. Verdu, A statistical theory of polymer network degradation, Polymer 55 (2014) 3811–3817.

[13] X. Colin, A. Mavel, C. Marais, Interaction between cracking and oxidation in organic matrix composites, J. Compos. Mater. 39 (2005) 1371–1389.

[14] E. Richaud, A. Guinault, S. Baiz, F. Nizeyimana, Epoxidized linseed oils based networks. Case of thermal degradation, Polym. Degrad. Stab. 166 (2019) 121–134.

[15] J.S. Arrieta, E. Richaud, B. Fayolle, F. Nizeyimana, Thermal oxidation of vinyl ester and unsaturated polyester resins, Polym. Degrad. Stab. 129 (2016) 142–155.

[16] M. Celina, J. Wise, D.K. Ottesen, K.T. Gillen, R.L. Clough, Oxidation profiles of thermally aged nitrile rubber, Polym. Degrad. Stab. 60 (1998) 493–504.

[17] T.G. Fox, P.J. Flory, Second-order transition temperatures and related properties of polystyrene. I. Influence of molecular weight, J. Appl. Phys. 21 (1950) 581–591.

[18] J.N. Cardenas, K.F. O'Driscoll, High-conversion polymerization. I. Theory and application to methyl methacrylate, J. Polym. Sci. 14 (1976) 883–897.

[19] O. Saito, Effects of high energy radiation on polymers II. End-linking and gel fraction, J. Phys. Soc. Jpn. 13 (1958) 1451–1464.

[20] G. Madras, J.M. Smith, B.J. McCoy, Degradation of Poly(methyl methacrylate) in Solution, Indus. Eng. Chem. Res. 35 (1996) 1795–1800.

[21] T. Kashiwagi, A. Inaba, J.E. Brown, K. Hatada, T. Kitayama, E. Masuda, Effects of weak linkages on the thermal and oxidative degradation of poly(methyl methacrylates), Macromolecules 19 (1986) 2160–2168.

[22] Y.-H. Hu, C.-Y. Chen, The effect of end groups on the thermal degradation of poly(methyl methacrylate), Polym. Degrad. Stab. 82 (2003) 81–88.

[23] M.Z. Bekanova, N.K. Neumolotov, A.D. Jablanović, A.V. Plutalova, E.V. Chernikova, Y.V. Kudryavtsev, Thermal stability of RAFT-based poly(methyl methacrylate): A kinetic study of the dithiobenzoate and trithiocarbonate end-group effect, Polym. Degrad. Stab. 164 (2019) 18–27.

[24] A. Inaba, T. Kashiwagi, J.E. Brown, Effects of initial molecular weight on thermal degradation of poly(methyl methacrylate): Part 1—Model 1, Polym. Degrad. Stab. 21 (1988) 1–20.

[25] M. Celina, K.T. Gillen, R.A. Assink, Review article: Accelerated aging and lifetime prediction: Review of non-Arrhenius behaviour due to two competing processes, Polym. Degrad. Stab. 90 (2005) 395–404.

[26] L. Achimsky, L. Audouin, J. Verdu, J. Rychly, L. Matisova-Rychla, On a transition at 80 °C in polypropylene oxidation kinetics, Polym. Degrad. Stab. 58 (1997) 283–289.

[27] D.M. Bate, R.S. Lehrle, A new approach for measuring the rate of pyrolysis of cross-linked polymers: evaluation of degradation rate constants for cross-linked PMMA, Polym. Degrad. Stab. 62 (1998) 67–71.

[28] Y. Nakamura, S. Yamago, Termination mechanism in the radical polymerization of methyl methacrylate and styrene determined by the reaction of structurally well-defined polymer end radicals, Macromolecules 48 (2015) 6450–6456.

[29] J.C. Bevington, H.W. Melville, R.P. Taylor, The termination reaction in radical polymerizations. Polymerizations of methyl methacrylate and styrene at 25°C, J. Polym. Sci. 12 (1954) 449–459.

[30] D.S. Achilias, C. Kiparissides, Development of a general mathematical framework for modeling diffusion-controlled free-radical polymerization reactions, Macromolecules 25 (1992) 3739–3750.

[31] F. Begum, S.L. Simon, Modeling methyl methacrylate free radical polymerization in nanoporous confinement, Polymer 52 (2011) 1539–1545.

[32] D.E. Roberts, Heats of polymerization. a summary of published values and their relation to structure, J. Res> Natl. Bur. Stand. (1950) 221–232 Research Paper RP2073 44.

[33] Y. Zhou, J. He, C. Li, L. Hong, Y. Yang, Dependence of thermal stability on molecular structure of RAFT/MADIX agents: a kinetic and mechanistic study, Macromolecules 44 (2011) 8446–8457.

[34] E.T. Denisov, I.B. Afanas'ev, Oxidation and Antioxidants in Organic Chemistry and Biology, Taylor & Francis, 2005.

[35] I. Higashide, K. Omata, Y. Nozawa, H. Yoshioka, Permeability to oxygen of poly(methy1 Methacrylate) films containing silane-treated glass flakes, J. Polym. Sci. Polym. Chem. Ed. 15 (1977) 2019–2028.

[36] E. Richaud, F. Farcas, P. Bartoloméo, B. Fayolle, L. Audouin, J. Verdu, Effect of oxygen pressure on the oxidation kinetics of unstabilised polypropylene, Polym. Degrad. Stab. 91 (2006) 398–405.

[37] K.U. Korcek, J.H.B. Chenier, J.A. Howard, K.U. Ingold, Absolute rate constants for hydrocarbon autoxidation. XXI. Activation energies for propagation and the correlation of propagation rate constants with carbon–hydrogen bond strengths, Revue canadienne de chimie 50 (1972) 2285–2297.

[38] K.T. Gillen, J. Wise, R.L. Clough, General solution for the basic autoxidation scheme, Polym. Degrad. Stab. 47 (1995) 149–161.

[39] J. Song, C.-H. Fischer, W. Schnabel, Thermal oxidative degradation of poly(methyl methacrylate), Polym. Degrad. Stab. 36 (1992) 261–266.

[40] B. Akih-Kumgeh, J.M. Bergthorson, Structure-reactivity trends of C1–C4 alkanoic acid methyl esters, Combust. Flame 158 (2011) 1037–1048.

[41] X. Colom, T. Garciá, J.J. Suñol, J. Saurin, F. Carrasco, Properties of PMMA artificially aged, J. Non-Crystal. Solid. 287 (2001) 308–312.

[42] R. Broska, N.C. Billingham, P.K. Fearon, Accelerating effect of poly(methyl methacrylate) on rubber oxidation, Part 1: A chemiluminescence study, Polym. Degrad. Stab. 93 (2008) 1100–1108.